Available online at www.sciencedirect.com

ScienceDirect

Advances in Space Research 70 (2022) 3249–3256

ADVANCES IN SPACE RESEARCH (a COSPAR publication)

www.elsevier.com/locate/asr

Effect of electron irradiation on polyimide composites based on track membranes for space systems

N.I. Cherkashina [a,*], V.I. Pavlenko [a], A.V. Noskov [b], D.S. Romanyuk [a], R.V. Sidelnikov [a], N.V. Kashibadze [a]

[a] Belgorod State Technological University named after V.G. Shoukhov, Kostyukov str., 46, Belgorod 308012, Russia
[b] Belgorod State National Research University, Pobedy str., 85, Belgorod 308015, Russia

Received 7 March 2022; received in revised form 7 July 2022; accepted 19 July 2022
Available online 22 July 2022

Abstract

The paper presents data on the resistance to electron irradiation of polyimide (PI) composite with nano-sized lead filler. PI composite with nano-filler were obtained on the basis of PI track membranes by electrochemical deposition of nano lead into the pores of track membranes. SEM-images, physical–mechanical and dielectric characteristics of PI composite with 70 wt% content of lead filler were examined. The composite was irradiated with 1–5 MeV electrons, and the maximum cumulative dose was 10 MGy. The effective range of an electron in a PI is greater than in a composite based on track membranes at the same initial electron energy: at E = 2 MeV - by 2.08 times, and at E = 5 MeV by 2.33 times.

Keywords: Polyimide; Polymer composite; Track membranes; Electron irradiation; Effective range

1. Introduction

Due to the high physical, mechanical and dielectric properties of polyimide (PI), materials based on it are widely used in industry. The high thermal and radiation resistance of PI allows it to be used even in extreme outer space conditions (Gouzman, 2019). Thermoregulatory coatings for spacecraft, elements of satellite antennae, electrical insulating materials, etc. are made of PI (Banks et al., 2004; Muthulakshmi et al., 2021; Gagliani and Supkis, 1980). However, with a prolonged stay in space, the functional characteristics of PI materials are significantly reduced. The impact of the space environment, which can damage polymeric materials including PI materials, includes electron and proton radiation, vacuum ultraviolet radiation, temperature effects, and atomic oxygen in low Earth orbit (Pavlenko et al., 2013, 2019; Gao et al., 2017; Cherkashina and Pavlenko, 2018a; Zhang, 2021a). Irradiation of PI with protons and electrons can lead to ionization and displacement effects, inducing structural damage and property degradation in polymeric materials (Li et al., 2007; Yue et al., 2016). Kang et al. (2008) and Mishra et al. (2003) reported on the structural transformations of PI, such as chain breaking and crosslinking under electron irradiation. Such transformations lead to changes in the optical, electrical, and mechanical properties of PI (Dong et al., 2018; Yoon et al., 2021; Abdul Majeed et al., 2021). To increase the resistance of PI to the effects of outer space, it is possible to introduce special fillers into the PI matrix (Shivakumar et al., 2020; Zhang et al., 2021b).

Much research has been devoted to the creation of functional PI nanocomposites with various fillers (Duan et al.,

* Corresponding author.
E-mail addresses: natalipv13@mail.ru, cherkashina.ni@bstu.ru (N.I. Cherkashina).

https://doi.org/10.1016/j.asr.2022.07.051
0273-1177/

2022; Wang et al., 2018; Liu et al., 2019; Su et al., 2017; Wozniak et al., 2016). Wang et al. (2022) succeeded in synthesizing PI/aminoquinoline-functionalized graphene oxide (PI/AQL-GO) nanocomposites. The synthesized nanocomposites have a low dielectric constant (2.96 @ 1 MHz) even with the addition of 0.5 wt% AQL-GO. However, Li et al. (2022) found that the introduction of $BaTiO_3$ nanoparticles into PI significantly increased the dielectric constant.

Morimune-Moriya et al. (2021) reported on the development of PI nanocomposites with nanodiamonds. Introduction of 0.1 wt% of nanodiamonds made it possible to increase the Young's modulus of PI composites by 70 %. Mekuria et al. (2021) synthesized composite films of PI with the inclusion of nanoparticles of silicon nitride modified by the amino group (Si_3N_4). Compared to the neat PI, the PI/Si_3N_4 nanocomposites exhibited a very high improvement in the tensile strength as well as Young's modulus, up to 105.4 % and 138.3 %, respectively.

In most cases, PI nanocomposites are obtained via an in situ polymerization technique (Yuen et al., 2008; Hamciuc et al., 2021; Zou et al., 2020). This is a rather laborious process. Therefore, the cost of such composites is high and production on an industrial scale is difficult. Another way to obtain PI composites is by mixing a PI press powder with highly dispersed fillers followed by further heating and pressing (Panin et al., 2021; Mu et al., 2015; Cherkashina and Pavlenko, 2018b; Kim and Nam, 2012). However, with this mixing method, it is impossible to achieve uniform distribution of the nanofiller. When introduced into the composite, nanofiller particles are strongly aggregated, which significantly affects the functional properties of the composite.

Cherkashina et al. (2020a) have previously developed a technique for obtaining nanocomposite films based on track (nuclear) membranes. Track (nuclear) membranes are films with nanopores. Such membranes are obtained by bombarding the polymer with heavy ions which leave their traces in the polymer - tracks. Chemical treatment of the film is carried out to obtain the required nanopore size (Dutt et al., 2021; Awad et al., 2020; Kutuzau et al., 2019; Wang et al., 2018; Kakitani et al., 2018). The authors synthesized PI nanocomposite films based on PI track membranes filled with nano-dispersed lead. In previous works, the high resistance of the developed nanocomposites to X-ray and gamma radiation was established (Cherkashina et al., 2020b; Cherkashina et al., 2021). This work presents data on the stability of nanocomposite based on PI track membranes filled with nano-dispersed lead to electron irradiation.

2. Materials and methods

2.1. Synthesis of composites

The synthesis of polymer composite with nano-dispersed lead was carried out by filling nanopores of PI track membranes with metallic lead. We used PI track membranes (manufactured by It4Ip, Louvain-la-Neuve, Belgium). The SEM-images of the PI track membranes is shown in Fig. 1. The pore diameter was 200 nm, the pore density was 5×10^8 cm^{-1}, and the thickness of one track membrane was 25 μm. The pores were located perpendicular to the membrane surface. The filling of pores in the nanometer range was carried out by electrodeposition of metallic nanoplate from an electrolyte solution based on lead tetrafluoroborate Pb $(BF_4)_2$. For electrodeposition, a lead coating 210 nm thick was preliminarily applied to one of the sides of the track membrane. During electrodeposition, the lead coating served as a cathode. A 210 μm thick lead layer remains and is an integral part of the composite.

The synthesis of the PI nanocomposite is presented in more detail in (Cherkashina et al., 2020a). The composite contained about 70 wt% nano-dispersed lead.

To assess the effect of a nanolead filler on PI, a comparison was made in this work with a pure PI film. We used PI film grade PMA 25 (LLC IZOTEKS, Russia). The thickness of the film, as well as that of the track membrane, was 25 μm.

2.2. Electron irradiation

The samples were irradiated with fast electrons with an energy of 1–5 MeV at a radiation sterilization unit with local biological shielding "Raduga" at the Federal Research and Production Center of the Moscow Radio Engineering Institute of the Russian Academy of Sciences (Tarasyuk, et al, 2017). The installation includes a microwave generator, a biosecurity housing, an electron accelerator, a modulator, and a number of supporting systems (vacuum, cooling, power supply, automated monitoring, and control).

The samples were irradiated in the one-sided irradiation mode. Before electron irradiation, the samples were thermally held in a vacuum oven at a temperature of 180 °C for 3 h. The electron beam power is 1.5 kW, the irradiation field uniformity is ± 5 %, the electron beam scanning frequency is 1–10 Hz, the beam current stability is ± 2.5 %, and the electron energy stability is ± 2.5 %. Specimen size: 25 × 150 mm (1 × 6 in.); jaw separation: 100 mm (4 in.); jaw speed: 50 mm/min (2 in./min).

To determine the distribution of the absorbed dose over the depth of materials and the effective range of electrons, tests were carried out with a constant increase in the thickness of the samples. For this purpose, PI (or PI composite) films 25 μm thick were tightly pressed against each other, and a detector was placed behind them. The effective range of electrons was determined by the total film thickness at which the detector did not detect radiation. The experiment was repeated for all studied energies (1–5 MeV). The total dose received by the each sample was 10 MGy.

After irradiation, the samples were placed in a desiccator filled with freshly dried silica gel and kept in the desic-

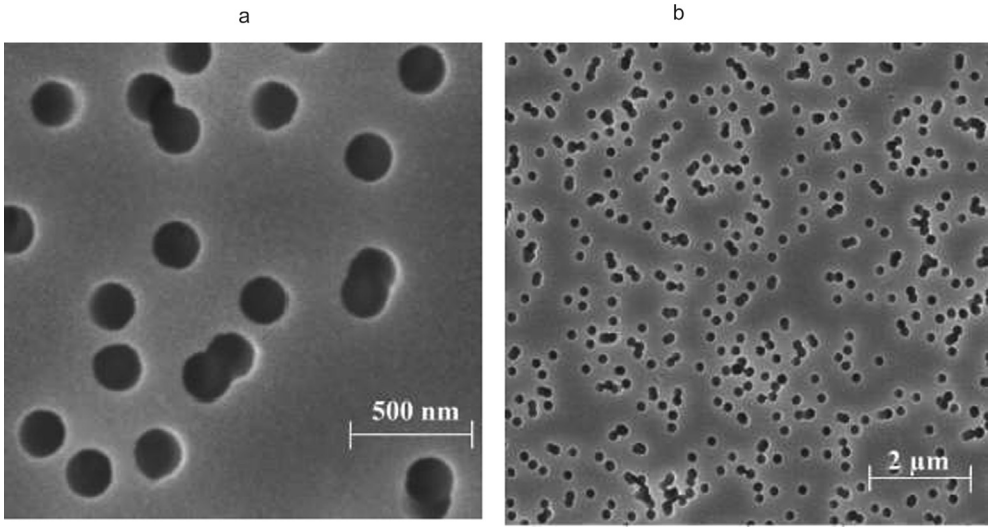

Fig. 1. SEM-images of pristine (un-irradiated) PI track membranes (TESCAN MIRA 3 LMU).

cator until studies were carried out to change the dielectric and physico-mechanical characteristics.

2.3. Research methods

To obtain SEM-images of materials before and after irradiation, a TESCAN MIRA 3 LMU field emission electron microscope (TESCAN, Czech Republic) was used.

The density of the samples was determined using standard methods according to ASTM D-1505–90 Test Method.

Strength characteristics such as tensile strength and elongation at break were determined using an Instron model 5882 universal testing machine (2007, Instron, USA). Tensile strength was determined using standard methods according to ASTM D-882–91 (Method A).

Volume resistivity was measured by placing a test specimen between two electrodes, applying a potential difference between them, and measuring the resulting current using a Keithley 6517B electrometer according to ASTM D-257.

The thermal conductivity coefficient of the samples was determined using the PIT-2.1 parting tool (2019, NPO Promavtomatika, Russia). The thermal conductivity coefficient was determined using standard methods according to ASTM F-433–77 (1987).

3. Results and discussion

3.1. Physical and mechanical properties of composites

Fig. 2 shows SEM images of the surface of a composite based on PI track membranes, the pores of which are filled with electrodeposited lead.

Analysis of SEM-images of the composite obtained on the basis of PI track membranes (Fig. 2 a, b) showed that

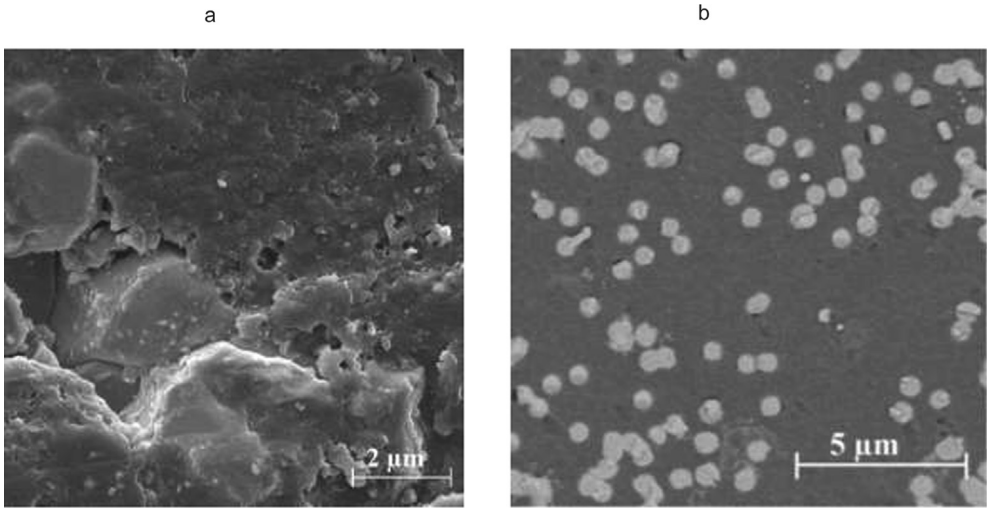

Fig. 2. SEM - images of the surface of a PI composite based on PI track membranes at various magnifications.

Table 1
Basic physical, mechanical and electrical characteristics of PI materials.

No	Characteristic	Indicators	
		Material	
		PI film	PI composite
1	Density, g/cm^3	1.43 ± 0.06	3.68 ± 0.07
2	Tensile strength, MPa	145.1 ± 4.3	98.0 ± 2.9
3	Elongation at break,%	72.0 ± 3.2	10.2 ± 1.2
4	Specific volumetric electrical resistance, Ohm•m	10^{16}	10^{3}
5	Thermal conductivity coefficient W/m • °C	0.2 ± 0.02	11.2 ± 0.5
6	Upper temperature limit, °C	350	250

when using this method of synthesis, the filler prticles - metallic lead - have the same dimension. The particle size of metallic lead depends on the size of the tracks in the membrane and is about 200 nm in cross section. When track (nuclear) membranes are used, metallic lead particles are evenly distributed throughout the entire volume of the composite, and the aggregation of lead particles is caused only by the overlap of tracks.

Table 1 shows the main physical, mechanical, and electrical characteristics of PI film and PI composites. The introduction of metallic lead into the PI film significantly increases the density of the composite.

The values of the mechanical characteristics of the composite are markedly reduced in comparison with pure PI film. Tensile strength of PI composite is 32 % lower in comparison with the pure PI film (Table 1). Since lead has low mechanical properties (Plumbridge and Gagg, 2000) it is not used as a construction material. Being a soft metal, lead cannot be used under conditions of friction, erosion, and other mechanical stresses. Therefore, the introduction of lead into PI significantly worsens the mechanical properties of the composites.

The introduction of metallic lead into the pores of the track membrane led to a decrease in the elongation at break by almost 7 times compared with a pure PI film. The introduction of nanolead had a huge impact on the electrical properties of the resulting composite compared to the original PI film: the specific volumetric electrical resistance decreased by 10^{13} times. The thermal conductivity coefficient of the PI composite is more than 50 times higher than that of pure PI film.

With the introduction of lead into PI film, the upper temperature limit of operation is significantly reduced. The upper temperature limit for the use of lead is 150 – 200 °C; at higher temperatures, it gradually begins to lose strength and corrosion resistance. For PI film this limit is 350 °C, and for PI composites it is 250 °C.

3.2. Impact of fast electrons

The experimental determination of the dose rate by depth of PI film and PI composite based on track membranes along the direction of electron irradiation is shown in Fig. 3. For all investigated materials irradiated with electrons of different energies, the same dose is achieved at a depth that, in approximation, is directly proportional to the electron energy in the 1–5 MeV region.

For both PI film and PI composite, an extreme distribution of the absorbed dose over the sample thickness is observed. It is noticeable that for electrons with an energy of 1–3 MeV, the absorbed dose distribution curve is rather narrow, and for electrons with an energy of 4–5 MeV, the maximum band broadens and covers deeper layers of the materials. The appearance of the maximum is associated with the development of the ionization process in the PI film bulk and PI composite caused by incident electrons, and an increase in the ionization density of the medium due to backscattering of secondary electrons at great depths (Pavlenko et al., 2010). This leads to an increase in the absorbed dose of electron radiation. The drop in the depth distribution curves of the absorbed dose is explained by the absorption and scattering of electrons.

Fig. 4 shows experimental data on the effective range of an electron in PI (tightly pressed layers of PI film) and PI composite (tightly pressed layers of track membranes filled with lead) depending on the initial electron energy up to 5 MeV. The data in Fig. 4 shows that the effective range for all materials is directly proportional to the initial energy of the electron, and increases with increasing energy. The penetration depth of an electron into PI is much greater than that of PI composite. It is known that the introduction of heavy fillers into polymers significantly increases their radiation-protective characteristics (Nikeghbal et al., 2020; Karabul and İçelli, 2021), which is what we observe in Fig. 4.

In addition, the improved radiation shielding characteristics of the composite based on track membranes as compared to the PI are related to the structure of the composites. When the track membrane comes into contact with metallic lead, a contact potential difference arises, which is determined by the difference between the work functions of the metal and the composite based on the track membrane. The work function in the composite based on the track membrane is higher than in the metal, therefore, the electron flux from the metal in the composite based on the track membrane will be greater and a positive charge will appear in the near-contact region of the metal, and a negative charge in the near-contact region of the

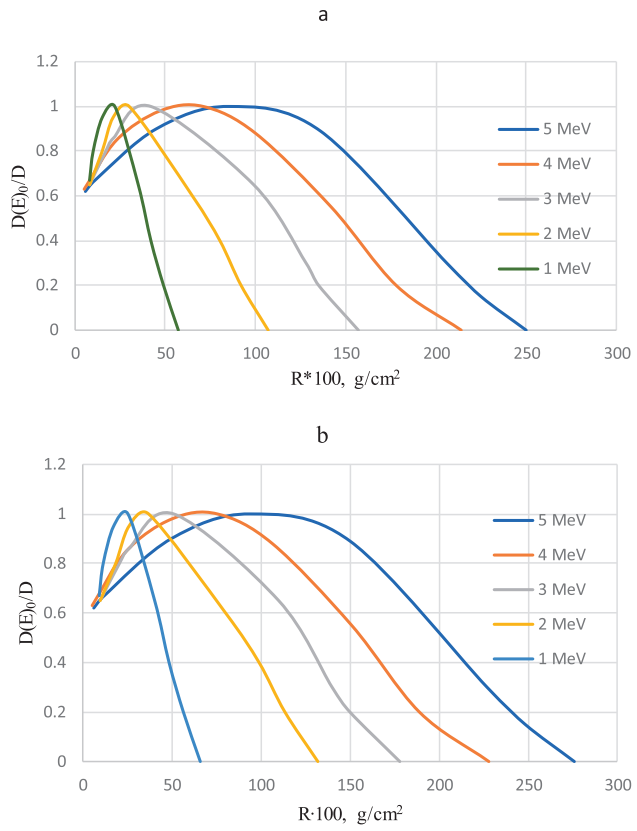

Fig. 3. Distribution of the absorbed dose over the depth of PI film (a) and PI composite (b).

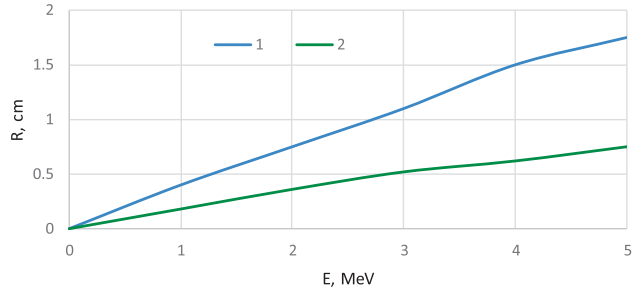

Fig. 4. Effective range of an electron in PI (1) and PI composite (2).

composite based on the track membrane. This leads to the appearance of a contact potential difference and to the appearance of an electric field, which prevents the transition of electrons from the metal in the composite based on the track membrane. The penetration depth of the field will depend on the concentration of electrons in the metal and the composite based on the track membrane, which can vary greatly. Since the concentration of electrons in the metal is much higher than in the composite based on the track membrane, the resulting contact electric field will only penetrate deeply into the composite based on the track membrane, while the near-contact layer of the composite based on the track membrane will increase which leads to an increase in the conductivity of the near-contact semiconductor layer.

For high-energy electrons incident on the considered layered structure, an increase in the electron density in the near-contact layer of a composite based on a track membrane leads to a significant increase in the probability of scattering at a larger angle in this layer, in particular, in the opposite direction. The ionization and radiation losses of electrons also increases. All this leads to a significant weakening of the electron flux in the PI composite based on track membranes.

3.3. Radiation resistance of materials

Figure 5 shows the data on the change in the mechanical characteristics of the materials under study after electron irradiation, depending on the energy. The total dose received by the each sample was 10MGy; the electron energy varied from 1 to 5 MeV.

An analysis of the data obtained on the change in the tensile strength characteristics of the materials under study showed that PI film and it composite are highly resistant to electron irradiation at an accumulated dose of 10 MGy in the considered energy range from 1 to 5 MeV (Figure 5). When PI film is irradiated, its tensile strength decreases by 4.8 % and 9.6 % at electron energies of 3 and 5 MeV, respectively. For a composite a decrease in tensile strength

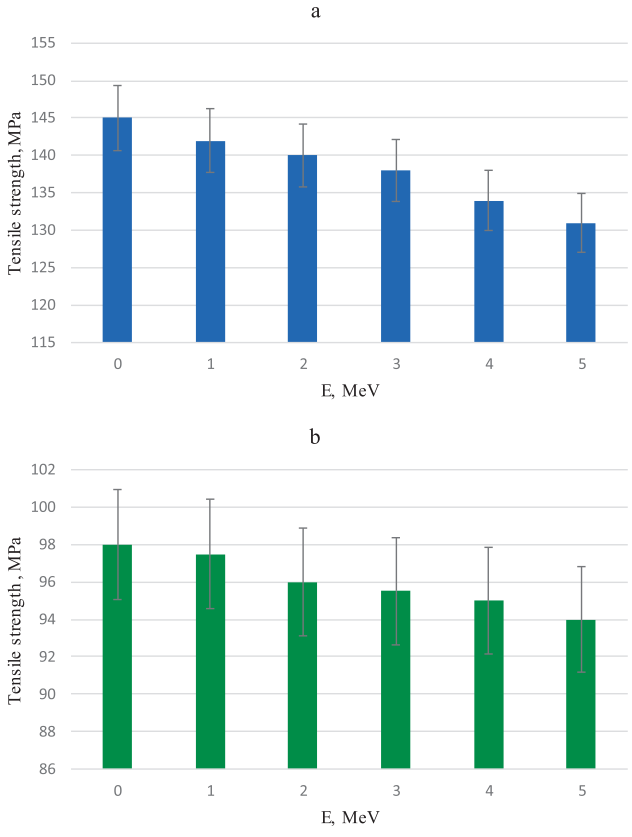

Fig. 5. Tensile strength of PI film (a) and PI composite (b) after irradiation as a function of energy at an accumulated dose of 10 MGy.

Table 2
Electrical characteristics of PI materials before and after electron irradiation (E = 5 MeV, D = 10 MGy).

No	Material	Specific volumetric electrical resistance, Ohm•m	
		Before irradiation	After irradiation
1	PI film	10^{16}	$4{,}5 \cdot 10^{15}$
2	PI composite based on track membranes	10^{3}	10^{3}

by 2.5 % and 4.1 % is observed at electron energies of 3 MeV and 5 MeV, respectively. In this case, most of the values fall into the confidence interval, taking into account the experimental error, therefore it can be argued that irradiation with electrons up to a dose of 10 MGy has practically no effect on the mechanical characteristics of the materials under study.

It is known that PI is the most radiation-resistant polymer. The radiation resistance of PI films (decrease in mechanical properties by a factor of 2) reaches 100 MGy (Wündrich, 1984; Coenen, 1995; Engelhart et all., 2018). Sasuga et al. (1985) reported ~ 30 % decrease in tensile strength, ~ 80 % decrease in elongation at break, and ~ 8 % increase in Young's modulus for PI irradiated with 2 MeV electron beam to a dose of 120 MGy.

The effect of electron irradiation of PI film and materials based on the change in electrical properties was investigated. Table 2 presents data on the change in the specific volumetric electrical resistance of the materials under study at an irradiation energy of 5 MeV and an accumulated dose of 10 MGy. It can be seen that irradiation of PI film led to a slight decrease in the specific volumetric electrical resistance, while irradiation of the composite did not affect the electrical properties. The results obtained agree with the literature data. Plis et al. (2019) have recently shown that the electrical conductivity of PI irradiated with electrons with an energy of 90 keV increased by two orders of magnitude after irradiation with a dose of 20 MGy, and with a subsequent increase for high doses.

4. Conclusions

The high resistance of PI film and PI composite with nano-sized lead filler to electron radiation with energies up to 5 MeV has been established. The use of PI track membranes leads to a uniform distribution of the lead filler, no aggregation of nano-dispersed lead filler is observed.

The effective range of an electron in a PI film is greater than in a composite based on track membranes at the same initial electron energy: at E = 2 MeV - by 2.08 times, and at E = 5 MeV by 2,33 times.

When PI film is irradiated, its tensile strength decreases by 4.8 % and 9.6 % at electron energies of 3 and 5 MeV, respectively. For a composite a decrease in tensile strength by 2.5 % and 4.1 % is observed at electron energies of 3 MeV and 5 MeV, respectively.

The developed composite based on PI track membranes and nanodispersed lead can be used for protection against cosmic radiation, since it has flexibility and high protective characteristics with respect to electron radiation.

Declaration of Competing Interest

The authors declare that they have no known competing financial interests or personal relationships that could have appeared to influence the work reported in this paper.

Acknowledgements

The work was supported by a project of the Russian Science Foundation, Russia (№19-79-10064). The work is realized using equipment of High Technology Center at BSTU named after V.G. Shukhov.

References

Abdul Majeed, R.M.A., More, S.E., Phatangare, A.B., et al., 2021. Synergetic effects of 1 MeV electron irradiation on the surface erosion in polyimide by atomic oxygen. Nucl. Instrum. Methods Phys. Res. B 490, 49–54. https://doi.org/10.1016/j.nimb.2020.12.021.

Awad, E.M., Hassan, S., Bebers, E., et al., 2020. Strong etching investigation on PADC CR-39 as a thick track membrane with deep depth profile study. Radiat. Phys. Chem. 177. https://doi.org/10.1016/j.radphyschem.2020.109104 109104.

Banks, B.A., Snyder, A., Miller, S.K., et al., 2004. Atomic-oxygen undercutting of protected polymers in low earth orbit. J. Spacecraft Rockets 41, 335–339. https://doi.org/10.2514/1.10726.

Cherkashina, N.I., Pavlenko, A.V., 2018a. Modification of optical characteristics of a polymer composite material under irradiation. Tech. Phys. 63, 571–575. https://doi.org/10.1134/S1063784218040072.

Cherkashina, N.I., Pavlenko, A.V., 2018b. Synthesis of polymer composite based on polyimide and $Bi_{12}SiO_{20}$ Sillenite. Polym. Plast. Technol. Eng. 57, 1923–1931. https://doi.org/10.1080/03602559.2018.1447129.

Cherkashina, N.I., Pavlenko, V.I., Manaev, V.A., et al., 2020a. Multilayer coatings based on polyimide track membranes and nanodispersed lead. Prog. Org. Coat. 138. https://doi.org/10.1016/j.porgcoat.2019.105432 105432.

Cherkashina, N.I., Pavlenko, V.I., Noskov, A.V., et al., 2020b. Using multilayer polymer PI/Pb composites for protection against X-ray bremsstrahlung in outer space. Acta Astronaut. 170, 499–508. https://doi.org/10.1016/j.actaastro.2020.02.022.

Cherkashina, N.I., Pavlenko, V.I., Noskov, A.V., et al., 2021. Gamma radiation attenuation characteristics of composites based on polyimide track membranes filled with nanodispersed Pb. Prog. Nucl. Energy 141. https://doi.org/10.1016/j.pnucene.2021.103959 103959.

Coenen, S., 1995. Radiation effects on polymers, SCK•CEN, Mol, Belgium, Réf. 27/95 - 134/SC.

Dong, S.-S., Shao, W.-Z., Yang, L., et al., 2018. Microstructure evolution of polyimide films induced by electron beam irradiation-load coupling treatment. Polym. Degrad. Stab. 155, 230–237. https://doi.org/10.1016/j.polymdegradstab.2018.07.020.

Duan, C., Gao, C., Li, S., et al., 2022. Tailoring polyimide composites with low friction and wear at high temperatures. J. Appl. Polym. Sci. 139, 51736. https://doi.org/10.1002/app.51736.

Dutt, S., Apel, P., Lizunov, N., et al., 2021. Shape of nanopores in track-etched polycarbonate membranes. J. Membr. Sci. 638. https://doi.org/10.1016/j.memsci.2021.119681 119681.

Engelhart, D.P., Plis, E., Cooper, R., et al., 2018. Effect of electron bombardment on polyimide film. Key Eng. Mater. 759, 48–53. https://doi.org/10.4028/www.scientific.net/kem.759.48.

Gagliani, J., Supkis, D.E., 1980. Non-flammable polyimide materials for aircraft and spacecraft applications. Acta Astronaut. 7, 653–683. https://doi.org/10.1016/0094-5765(80)90051-X.

Gao, H., Lan, X., Liu, L., et al., 2017. Study on performances of colorless and transparent shape memory polyimide film in space thermal cycling, atomic oxygen and ultraviolet irradiation environments. Smart. Mater. Struct. 26 (9) 095001.

Gouzman, I., Grossman, E., Verker, R., 2019. Advances in polyimide-based materials for space applications. Adv. Mater. 31, 1807738. https://doi.org/10.1002/adma.201807738.

Hamciuc, C., Asandulesa, M., Hamciuc, E., et al., 2021. Novel polyimide/copper-nickel ferrite composites with tunable magnetic and dielectric properties. Polymers 13 (10), 1646. https://doi.org/10.3390/polym13101646.

Kakitani, K., Koshikawa, H., Yamaki, T., et al., 2018. Preparation of conductive layer on polyimide ion-track membrane by Ar ion implantation. Surf. Coat. Technol. 355, 181–185. https://doi.org/10.1016/j.surfcoat.2018.05.057.

Kang, P.-H., Jeon, Y.-K., Jeun, J.-P., et al., 2008. Effect of electron beam irradiation on polyimide film. J. Ind. Eng. Chem. 14, 672–675. https://doi.org/10.1016/j.jiec.2008.03.004.

Karabul, Y., İçelli, O., 2021. The assessment of usage of epoxy based micro and nano-structured composites enriched with Bi_2O_3 and WO_3 particles for radiation shielding. Results Phys. 26. https://doi.org/10.1016/j.rinp.2021.104423 104423.

Kim, H.J., Nam, S.M., 2012. Powder preparation in aerosol deposition for Al_2O_3-polyimide composite thick films. Electron. Mater. Lett. 8, 65–70. https://doi.org/10.1007/s13391-011-0810-7.

Kutuzau, M., Kozlovskiy, A., Borgekov, D., et al., 2019. Optimization of PET ion-track membranes parameters. Mater. Today: Proc. 7, 866–871. https://doi.org/10.1016/j.matpr.2018.12.086.

Li, R., Li, C., He, S., et al., 2007. Radiation effect of keV protons on optical properties of aluminized Kapton film. Radiat. Phys. Chem. 76, 1200–1204. https://doi.org/10.1016/j.radphyschem.2006.12.005.

Li, Z., Wang, X., Hu, Y., et al., 2022. Triboelectric properties of $BaTiO_3$/polyimide nanocomposite film. Appl. Surf. Sci. 572. https://doi.org/10.1016/j.apsusc.2021.151391 151391.

Liu, X., Ji, T., Li, N., et al., 2019. Preparation of polyimide composites reinforced with oxygen doped boron nitride nano-sheet as multifunctional materials. Mater. Des. 180. https://doi.org/10.1016/j.matdes.2019.107963 107963.

Mekuria, T.D., Wang, L., Zhang, C., et al., 2021. Synthesis and characterization of high strength polyimide/silicon nitride nanocomposites with enhanced thermal and hydrophobic properties. Chin. J. Chem. Eng. 32, 446–453. https://doi.org/10.1016/j.cjche.2020.09.066.

Mishra, R., Tripathy, S.P., Dwivedi, K.K., et al., 2003. Spectroscopic and thermal studies of electron irradiated polyimide. Radiat. Meas. 36, 621–624. https://doi.org/10.1016/S1350-4487(03)00212-9.

Morimune-Moriya, S., Obara, K., Fuseya, M., et al., 2021. Development and characterization of strong, heat-resistant and thermally conductive polyimide/nanodiamond nanocomposites. Polym. 230. https://doi.org/10.1016/j.polymer.2021.124098 124098.

Mu, L., Zhu, J., Fan, J., et al., 2015. Self-Lubricating Polytetrafluoroethylene/Polyimide Blends Reinforced with Zinc Oxide Nanoparticles. J. Nanomater. Volume 2015, Article ID 545307. http://dx.doi.org/10.1155/2015/545307.

Muthulakshmi, B., Hanumanth Rao, C., Sharma, S.V., 2021. Application of non-woven aramid-polyimide composite materials for high reliability printed circuit boards for use in spacecraft electronics. Mater. Today: Proc. 40, S254-S257. https://doi.org/10.1016/j.matpr.2021.02.221.

Nikeghbal, K., Zamanian, Z., Shahidi, S., et al., 2020. Designing and fabricating nano-structured and micro-structured radiation shields for protection against CBCT exposure. Materials 13, 4371. https://doi.org/10.3390/ma13194371.

Panin, S.V., Luo, J., Buslovich, D.G., et al., 2021. Experimental–FEM study on effect of tribological load conditions on wear resistance of three-component high-strength solid-lubricant PI-based composites. Polymers 13, 2837. https://doi.org/10.3390/polym13162837.

Pavlenko, V.I., Cherkashina, N.I., 2019. Effect of SiO_2 crystal structure on the stability of polymer composites exposed to vacuum ultraviolet radiation. Acta Astronaut. 155, 1–9. https://doi.org/10.1016/j.actaastro.2018.11.017.

Pavlenko, V.I., Yastrebinskiy, R.N., Edamenko, O.D., et al., 2010. Affecting of high-power bunches of rapid electrons polymeric radiation-protective kompozity. Problems Atomic Sci. Technol. 1, 129–134.

Pavlenko, V.I., Novikov, L.S., Bondarenko, G.G., et al., 2013. Experimental and physicomathematical simulation of the effect of an incident flow of atomic oxygen on highly filled polymer composites. Inorg. Mater. Appl. Res. 4, 169–173. https://doi.org/10.1134/S2075113313020135.

Plis, E.A., Engelhart, D.P., Cooper, R., et al., 2019. Review of radiation-induced effects in polyimide. Appl. Sci. 9, 1999. https://doi.org/10.3390/app9101999.

Sasuga, T., Hayakawa, N., Yoshida, K., et al., 1985. Degradation in tensile properties of aromatic polymers by electron beam irradiation. Polym. 86, 1039–1045. https://doi.org/10.1016/0032-3861(85)90226-5.

Shivakumar, R., Bolker, A., Tsang, S.H., et al., 2020. POSS enhanced 3D graphene - polyimide film for atomic oxygen endurance in Low Earth Orbit space environment. Polym. 191. https://doi.org/10.1016/j.polymer.2020.122270 122270.

Su, C., Xue, F., Li, T., et al., 2017. Fabrication and multifunctional properties of polyimide based hierarchical composites with in situ grown carbon nanotubes. RSC Adv. 7, 29686–29696. https://doi.org/10.1039/C7RA00436B.

Tarasyuk, V.T., Semkina, A.A. Filippovich, V.P., et al., 2017. The Study of Electron Irradiation Effect on Multilayer Polymer Materials before and after Storage for One Year, Conference: 12th International Scientific Workshop in Memory of Professor V.P. Sarantsev "Problems of Colliders and Charged Particle Accelerators" At: Alushta, 2017. 2017 http://dx.doi.org/10.13140/RG.2.2.18576.84485.

Wang, T., Wang, M., Fu, L., et al., 2018. Enhanced thermal conductivity of polyimide composites with boron nitride nanosheets. Sci. Rep. 8, 1557. https://doi.org/10.1038/s41598-018-19945-3.

Wang, T., Li, J., Niu, F., et al., 2022. Low-temperature curable and low-dielectric polyimide nanocomposites using aminoquinoline-functionalized graphene oxide nanosheets. Compos. B. Eng. 228. https://doi.org/10.1016/j.compositesb.2021.109412 109412.

Wang, P., Wang, X., Ling, Y., et al., 2018. Ultrafast selective ionic transport through heat-treated polyethylene terephthalate track membranes with sub-nanometer pores. Radiat. Meas. 119, 80–84. https://doi.org/10.1016/j.radmeas.2018.09.007.

Wozniak, A.I., Ivanov, V.S., Kosova, O.V., et al., 2016. Thermal properties of polyimide composites with nanostructured silicon carbide. Orient. J. Chem. 32, 2967–2974. https://doi.org/10.13005/ojc/320616.

Wündrich, K., 1984. A review of radiation resistance for plastic and elastomeric materials, Radiat. Phys. Chem (1977). 24, 503-510. https://doi.org/10.1016/0146-5724(84)90185-7.

Yoon, H., Kim, B.H., Kwon, S.H., et al., 2021. Polyimide photodevices without a substrate by electron-beam irradiation. Appl. Surf. Sci. 570. https://doi.org/10.1016/j.apsusc.2021.151185 151185.

Yue, L., Wu, Y., Sun, C., et al., 2016. Effects of proton pre-irradiation on radiation induced conductivity of polyimide. Radiat. Phys. Chem. 119, 130–135. https://doi.org/10.1016/j.radphyschem.2015.09.019.

Yuen, S.-M., Ma, C.-C. M., Chiang, C.-L., et al., 2008. Morphology and Properties of Aminosilane Grafted MWCNT/Polyimide Nanocom-

posites. J. Nanomater. Volume 2008, Article ID 786405. https://doi.org/10.1155/2008/786405.

Zhang, Y., Wu, H., Guo, Y.-D., et al., 2021a. Atomic oxygen-resistant polyimide composite films containing nanocaged polyhedral oligomeric silsesquioxane components in matrix and fillers. Nanomaterials 11, 141. https://doi.org/10.3390/nano11010141.

Zhang, Y., Yan, H., Xu, P., et al., 2021b. A novel POSS-containing polyimide: synthesis and its composite coating with graphene-like MoS_2 for outstanding tribological performance. Prog. Org. Coat. 151. https://doi.org/10.1016/j.porgcoat.2020.106013 106013.

Zou, K., Fan, Z., He, C., et al., 2020. High-temperature energy storage properties in polyimide-based nanocomposites filled with antiferroelectric nanoparticles. J. Mater. Res. Technol. 9, 11344–11350. https://doi.org/10.1016/j.jmrt.2020.08.030.